Iterative Soft-Detection of Space-Time-Frequency Shift Keying

Hoang Anh Ngo†, Shinya Sugiura‡ and Lajos Hanzo†
† School of Electronics & Computer Science, University of Southampton, UK
‡ Toyota Central R&D Labs., Inc., Japan
Email: †{han08r, lh}@ecs.soton.ac.uk; ‡sugiura@mosk.tytlabs.co.jp

***Abstract*— Inspired by the concept of Space-Time Shift Keying (STSK), the further evolved philosophy of Space-Time-Frequency Shift Keying (STFSK) was proposed for Multiple-Input-Multiple-Output (MIMO) wireless communications, where a beneficial diversity gain may be gleaned from three different domains, namely the space-, time- and frequency-domain. In this paper we proposed soft-detected STFSK in order to conceive its iterative decoding aided version combined with channel codes. Our results showed that the STFSK soft demodulator, which iteratively exchanges *extrinsic* information with channel codes, may decrease the required transmit power by approximately 3 dB at the E_b/N_0 of 10^{-5}, compared to hard-decision STFSK. Furthermore, the detection complexity of both the hard- and the soft-decision STFSK demodulator is quantified in terms of the number of multiplications and additions required for each detection iteration.**

I. Introduction

The family of multiple-input-multiple-output (MIMO) arrangements, one of the most significant technical breakthroughs in contemporary communications, has attracted substantial research attention owing to its potential to increase the attainable capacity without requiring additional bandwidth. A simple diversity-gain-oriented detection technique is constituted by the employment of multiple antennas at the receiver, where several diversity combining techniques can be utilized in order to exploit the independently fading signal replicas. Similarly, MIMO techniques additionally employing multiple transmit - rather than only receive-antennas - have also been proposed in the literature [1]–[4]. In [1], Alamouti proposed a simple transmit diversity technique employing two-transmit antenna. Inspired by this proposal, Tarokh *et al.* further developed the technique, creating the fully-fledged family of Space-Time Block Codes (STBC) [3], [4]. The STBCs are capable of maximizing the attainable diversity order, but offer no coding gain. By contrast, the family of Space-Time Trellis Codes (STTC) [2] is capable of providing both diversity gain and coding gain at the cost of an increased decoding complexity. Furthermore, Hochwald *et al.* proposed the attractive transmit diversity concept of the Space-Time Spreading [5] for the downlink of Wideband Code Division Multiple Access (WCDMA), which is capable of achieving the highest possible diversity gain. However, unfortunately all of the above-mentioned codes fail to attain a multiplexing gain.

In contrast to space-time coding, the class of spatial division multiplexing, such as the family of BLAST schemes [6], [7], is capable of increasing the transmission rate, i.e the multiplexing gain, albeit this is achieved at the cost of significantly increasing the decoding complexity. For the sake of striking an attractive tradeoff between the attainable space-time coding and spatial multiplexing gains, Hassibi *et al.* proposed Linear Dispersion Codes (LDC) [8].

However, the above-mentioned MIMO arrangements have their own problems, for example due to imposing inter-antenna interference and inter-antenna synchronization errors. In order to avoid these problems, the philosophy of activating only a single transmit antenna at any instant was utilized by Haas and his team, proposing Spatial Modulation (SM) [9], while the team of Ghrayaeb and Szczecinski [10] introduced the Space Shift Keying (SSK) concept into MIMO communications. Motivated by the above concepts, the authors of [11] conceived Space-Time Shift Keying (STSK), which strikes an improved diversity versus multiplexing tradeoff. This design results in a reduced-complexity system operating at a higher capacity than the SM/SSK and BLAST schemes. As a further advance, we proposed the Space-Time-Frequency Shift Keying (STFSK)[1] concept [13], where a beneficial diversity gain may be gleaned from three different domains, namely the space-, time- and frequency-domain (SD, TD and FD). In addition to the advantages provided by STSK modulation, the STFSK scheme is capable of avoiding the Inter-Symbol Interference (ISI) imposed by frequency-selective fading channels.

In this paper we further develop the STFSK philosophy with the aid of iterative decoding in order to investigate the beneficial effects of these techniques on the performance of the holistically optimized system. The outline of this paper is as follows. Section II describes the system's architecture and the associated assumptions. The STFSK soft-demodulation and our EXtrinsic Information Transfer (EXIT) chart investigations are included in Section III. The detection complexity of STFSK demodulator is quantified in Section IV. Finally, the attainable system performance is presented in Section V, followed by our concluding remarks in Section VI.

II. Space-Time-Frequency Shift Keying

In this section, we will briefly describe the STFSK concept, which was detailed in [13]. Consider an $(M \times N)$-element system, where the transmitter and receiver employ M and N antennas, respectively. The channel is assumed to impose frequency-selective Rayleigh fading. Generally, a transmission block-based system model may be described as:

$$\boldsymbol{Y}_k(i) = \begin{cases} \sum\limits_{j=0}^{J-1} \boldsymbol{H}(i-j,j)\boldsymbol{S}(i-j) + \boldsymbol{V}(i) & : \; at\ transmit\ freq. \\ \overline{\boldsymbol{V}}(i) & : \; otherwise \end{cases} \tag{1}$$

where i indicates the block index and j represents the tap index in the tap-delay-line channel model, which consists of J taps. Naturally, flat fading is encountered for $J = 1$. Furthermore, $\boldsymbol{Y}_k \in \mathcal{C}^{N\times T}$ represents the received signals of the N antennas at the k^{th} frequency and $\boldsymbol{S} \in \mathcal{C}^{M\times T}$ denotes the signal transmitted from the M antennas in T time slots. Furthermore, $\boldsymbol{H}(i,j) \in \mathcal{C}^{N\times M}$ characterizes the coefficients of the i^{th} symbol at the j^{th} channel tap, each obeying correlated frequency-selective Rayleigh fading. Finally, $\boldsymbol{V}$ denotes the complex-valued zero-mean Gaussian distribution of $\mathcal{CN}(0, N_0)$, where N_0 is the noise variance. It is also assumed that the fading and noise coefficients remain constant during each time slot.

Fig. 1 illustrates the transmitter of the STFSK scheme, where the information bits are divided into three parallel bits streams. In the first bit stream each group of $log_2(q)$ bits is mapped to one out of

The research leading to these results has received funding from the European Union's Seventh Framework Programme [FP7/2007-2013] under grant agreement N^{o}214625. The financial support of RC-UK under the auspices of the UK-India Advanced Technology Centre and that of the China-UK Science Bridge in 4G Wireless Communications is also gratefully acknowledged.

[1]The design in [12] is a special case and referred to as SFSK in this paper.

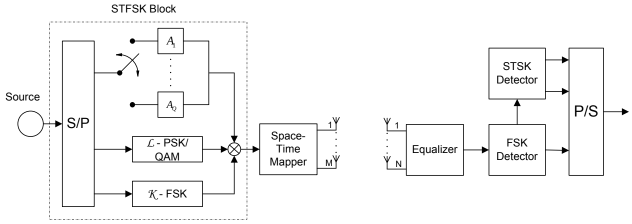

Fig. 1. The transceiver block diagram of STFSK scheme.

Q pre-defined dispersion matrices $\boldsymbol{A}_q \in \mathcal{C}^{M\times T}$ $(q = 1, 2, ..., Q)$. The second stream is mapped to $s_l(i)$ symbols $(l = 1, 2, ..., L)$ by a conventional modulation scheme, such as L-PSK or L-QAM, while the third one is mapped to the FSK symbol $r(i)$, which is represented by $r(i) = cos(2\pi f_r t + \varphi_r)$, where f_i $(r = 1, 2, ..., K))$ is the frequency associated with the i^{th} transmitted FSK symbol and φ_i is the random phase during the i^{th} symbol interval. Then, the resultant modulated streams are multiplexed in order to create the space-time-frequency block $\boldsymbol{S}(i) \in \mathcal{C}^{M\times T}$, which conveys a total of $log_2(QLK)$ source bits, yielding

$$\boldsymbol{S}(i) = r(i)s(i)\boldsymbol{A}(i), \tag{2}$$

where each symbol $s(i)$ is a function of time during the period T_s of each time slot.

As in [13], the space-time-frequency signal $\overline{\overline{\boldsymbol{Y}}}$ received at the destination may be presented as

$$\overline{\overline{\boldsymbol{Y}}}(i) = \{\overline{\boldsymbol{Y}}_1(i), \overline{\boldsymbol{Y}}_2(i), ..., \overline{\boldsymbol{Y}}_k(i), ..., \overline{\boldsymbol{Y}}_K(i)\}, \tag{3}$$

where we have

$$\overline{\boldsymbol{Y}}_k(i) = \begin{cases} \sum\limits_{j=0}^{J-1} \overline{\boldsymbol{H}}(i-j, j)\chi\boldsymbol{K}(i) + \overline{\boldsymbol{V}}(i-j) & : \ at\ transmit\ freq. \\ \overline{\boldsymbol{V}}(i) & : \ otherwise \end{cases} \tag{4}$$

with the variables formulated as

$$\begin{aligned} \bar{\boldsymbol{Y}} &= & vec(\boldsymbol{Y}) & \quad \in \mathcal{C}^{NT\times 1}, & (5)\\ \bar{\boldsymbol{H}} &= & \boldsymbol{I}\otimes\boldsymbol{H} & \quad \in \mathcal{C}^{NT\times MT}, & (6)\\ \bar{\boldsymbol{V}} &= & vec(\boldsymbol{V}) & \quad \in \mathcal{C}^{NT\times 1}, & (7)\\ \chi &= & [vec(\boldsymbol{A}_1)\cdots vec(\boldsymbol{A}_Q)] & \quad \in \mathcal{C}^{MT\times Q}, & (8) \end{aligned}$$

where $\boldsymbol{I}$ is the $(T \times T)$-element identity matrix and $\otimes$ is the Kronecker product. Furthermore, $\boldsymbol{K}(i) \in \mathcal{C}^{Q\times 1}$ is the equivalent transmitted signal vector, being expressed as

$$\boldsymbol{K}(i) = [\underbrace{0, \cdots, 0}_{q-1}, r(i)s(i), \underbrace{0, \cdots, 0}_{Q-q}]^T, \tag{9}$$

where ^{T} indicates the matrix transpose operation.

At the receiver, we employ an FSK demodulator consisting of a bank of K parallel square-law detectors [14] in order to detect the activated frequencies of the SFSK symbols. Then the maximum likelihood (ML) detector [15] is employed to search for an appropriate pair of the l^{th} $(l = 1, \cdots, L)$ PSK/QAM symbol and the q^{th} $(q = 1, \cdots, Q)$ dispersion matrix. More particularly, the estimate $(\hat{q}, \hat{l})$ is given by minimizing the following metric

$$\begin{aligned} (\hat{q}, \hat{l}) &= arg\min_{q,l} \Big|\Big| \bar{\boldsymbol{Y}}_k(i) - \bar{\boldsymbol{H}}(i)\chi\boldsymbol{K}_{q,l,k}(i) \\ &\quad - \sum_{j=1}^{J-1} \bar{\boldsymbol{H}}(i-j, j)\chi\boldsymbol{K}(i-j)\Big|\Big|^2 & (10)\\ &= arg\min_{q,l} \Big|\Big| \bar{\boldsymbol{Y}}_k(i) - r(i)s_l(i)\big(\bar{\boldsymbol{H}}(i)\chi\big)_q \\ &\quad - \sum_{j=1}^{J-1} \bar{\boldsymbol{H}}(i-j, j)\chi\boldsymbol{K}(i-j)\Big|\Big|^2, & (11) \end{aligned}$$

where $s_l(i)$ is the l^{th} symbol in the L-point constellation at the i^{th} block index and the signal vector $\boldsymbol{K}_{q,l,k}$ $(1 \le q \le Q, 1 \le l \le L, 1 \le k \le K)$ is presented by

$$\boldsymbol{K}_{q,l,k}(i) = [\underbrace{0, \cdots, 0}_{q-1}, r(i)s_l(i), \underbrace{0, \cdots, 0}_{Q-q}]^{Tr}. \tag{12}$$

Furthermore, $\sum_{j=1}^{J-1} \bar{\boldsymbol{H}}(i-j, j)\chi\boldsymbol{K}(i-j)$ represents the delayed paths of the dispersive channel, which is omitted in flat-fading environments, while $\big(\bar{\boldsymbol{H}}(i)\chi\big)_q$ denotes the q^{th} column of the matrix $\bar{\boldsymbol{H}}(i)\chi$.

Additionally, in order to maintain a unity transmission power for a STSK symbol duration, each of the Q dispersion matrices has to obey the power constraint of [11]

$$tr[\boldsymbol{A}_q^{\dagger}\boldsymbol{A}_q] = T \qquad (q = 1, \cdots, Q), \tag{13}$$

where $tr[\cdot]$ indicates the trace of a matrix, while the superscript $\dagger$ denotes the complex conjugate transpose operation.

When $K = 1$, the STFSK becomes the STSK scheme [11] while it becomes the SFSK [12], when $L = 1$.

III. Soft STFSK Demapper

Let us now detail the soft demapper designed for our STFSK schemes. Based on the equivalent system model of Eq. (3) derived for our STFSK scheme, the conditional probability $p(\overline{\overline{\boldsymbol{Y}}}|\boldsymbol{K}_{q,l,k})$ is obtained as

$$p(\overline{\overline{\boldsymbol{Y}}}|\boldsymbol{K}_{q,l,k}) = \frac{1}{(\pi N_0)^{NT}} \exp\left(-\frac{||\overline{\boldsymbol{Y}}_k - \overline{\boldsymbol{H}}\boldsymbol{\chi}\boldsymbol{K}_{q,l,k}||^2}{N_0}\right). \tag{14}$$

Note that the equivalent received signals $\overline{\boldsymbol{Y}}$ carry $B = log_2(KLQ)$ channel-coded binary bits $\boldsymbol{b} = [b_1, b_2, \cdots, b_B]$, where the resultant extrinsic LLR value of bit b_k for $k = 1, \cdots, B$ may be expressed as [16]

$$\begin{aligned} L_{\mathrm{e}}(b_k) &= \ln \frac{\sum\limits_{\boldsymbol{K}_{q,l,k}\in\boldsymbol{Z}_1^k} p(\overline{\boldsymbol{Y}}_k|\boldsymbol{K}_{q,l,k}) \cdot e^{\left[\sum_{j\neq k} b_j L_a(b_j)\right]}}{\sum\limits_{\boldsymbol{K}_{q,l}\in\boldsymbol{Z}_0^k} p(\overline{\boldsymbol{Y}}_k|\boldsymbol{K}_{q,l,k}) \cdot e^{\left[\sum_{j\neq k} b_j L_a(b_j)\right]}} & (15)\\ &= \ln \frac{\sum\limits_{\boldsymbol{K}_{q,l,k}\in\boldsymbol{Z}_1^k} e^{\left[\frac{-\left|\left|\overline{\boldsymbol{Y}}_k - \overline{\boldsymbol{H}}\boldsymbol{\chi}\boldsymbol{K}_{q,l,k}\right|\right|^2}{N_0} + \sum_{j\neq k} b_j L_a(b_j)\right]}}{\sum\limits_{\boldsymbol{K}_{q,l,k}\in\boldsymbol{Z}_0^k} e^{\left[\frac{-\left|\left|\overline{\boldsymbol{Y}}_k - \overline{\boldsymbol{H}}\boldsymbol{\chi}\boldsymbol{K}_{q,l,k}\right|\right|^2}{N_0} + \sum_{j\neq k} b_j L_a(b_j)\right]}}, \end{aligned}$$

where $\boldsymbol{Z}_1^k$ and $\boldsymbol{Z}_0^k$ represent the sub-space of the legitimate equivalent signals $\boldsymbol{Z}$, satisfying $\boldsymbol{Z}_1^k \equiv \{\boldsymbol{K}_{q,l,k} \in \boldsymbol{Z} : b_k = 1\}$ and $\boldsymbol{Z}_0^k \equiv \{\boldsymbol{K}_{q,l,k} \in \boldsymbol{Z} : b_k = 0\}$, respectively, while $L_a(\cdot)$ represents the *a priori* information expressed in terms of the LLRs of the corresponding bits. Furthermore, Eq. (15) is readily simplified by the max-log approximation [17], yielding:

$$\begin{aligned} L_{\mathrm{e}}(b_k) &= \max_{\boldsymbol{K}_{q,l,k}\in\boldsymbol{Z}_1^k} \left[-\frac{||\overline{\boldsymbol{Y}}_k - \overline{\boldsymbol{H}}\boldsymbol{\chi}\boldsymbol{K}_{q,l,k}||^2}{N_0} + \sum_{j\neq k} b_j L_a(b_j)\right] \\ &\quad - \max_{\boldsymbol{K}_{q,l,k}\in\boldsymbol{Z}_0^k} \left[-\frac{||\overline{\boldsymbol{Y}}_k - \overline{\boldsymbol{H}}\boldsymbol{\chi}\boldsymbol{K}_{q,l,k}||^2}{N_0} + \sum_{j\neq k} b_j L_a(b_j)\right]. \end{aligned} \tag{16}$$

EXIT Chart Analysis: The EXIT charts, proposed by S. ten Brink [16], constitute useful tools designed for the analysis of iterative decoding schemes. This tool allows designers to graphically explore the characteristics of a demodulator/decoder based on the soft-input soft-output decisions, which are exchanged between the decoder components. The chart describes the dependence of the

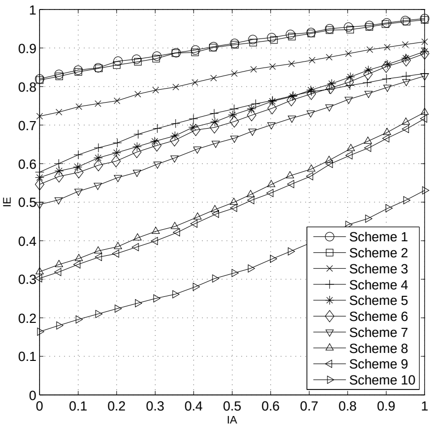

Fig. 2. The EXIT functions of the various STFSK schemes specified in Table II and using soft-demodulation of $B = log_2(K \times Q \times L) = 3$ bits/block.

extrinsic information on the *a-priori* information, which is typically quantified by the mutual information of the Log-Likelihood Ratios (LLR).

In EXIT chart analysis, the mutual information between the *a-priori* LLRs, L_A, or *extrinsic* LLRs, L_E, and the corresponding bits S may be computed as [16]

$$I(L_i; S) = \frac{1}{2} \sum_{s=\pm 1} \int_{-\infty}^{\infty} p_{L_i}(x|s) log \frac{p_{L_i}(x|s)}{p_{L_i}(x)} dx \qquad (i = A, E) \quad (17)$$

with

$$p_{L_i}(x) = \frac{1}{2} p_{L_i}(x|s = +1) + p_{L_i}(x|s = -1), \quad (18)$$

where $p_{L_i}(x|s)$ is the probability of the *a-priori* or *extrinsic* information conditioned on $s = \pm 1$. According to the amount of mutual information of L_A and L_E, the two EXIT functions (or EXIT curves), i.e. the inner and outer EXIT functions, may be drawn. The convergence characteristics of the iterative receiver may now be predicted by examining the relationship between the two curves of the EXIT chart.

The EXIT functions of the various STFSK schemes characterized in Table II are shown in Fig. 2, leading to the following observations:

- Increasing the number of frequencies, K, may increase the *extrinsic* information at the cost of extending the bandwidth used. This fact may be inferred by comparing Schemes 1,2,3 and 4, where we have K =16, 8, 4 and 2, respectively.
- Increasing the number of dispersion matrices, Q, reduces the *extrinsic* information, when the same number of frequencies, K, is employed, which may be observed by comparing Schemes 3, 6 and 8.

IV. Detection Complexity

Let us quantify the computational complexity imposed by the ML hard-detection and the soft-detection of STFSK schemes, which is given by the number of real-valued multiplications and real-valued additions. We make the following assumptions:

- Each complex-valued addition is equivalent to two real-valued additions.
- Each complex-valued multiplication is equivalent to four real-valued multiplications plus two real-valued addition.
- Each square of absolute value calculation carried out for a complex number is equivalent to two real-valued multiplication and one real-valued addition.

A. Hard Demodulator

1) STFSK: First, we consider the complexity of the FSK detector. If the square-law FSK detector is employed as mentioned in Sec. II, then the number of multiplications, $C^{\times}$, and the number of additions, C^{+}, may be obtained as

$$C^{\times} = 2K, \quad (19)$$
$$C^{+} = K. \quad (20)$$

In order to evaluate the complexity of the STSK detector, Eq. (10) can be utilized, where the product of $\chi \boldsymbol{K}$ involves the multiplication of two matrices, where one has a dimension of $(n_T \times Q)$, which the other has a dimension of $(Q \times 1)$. However, the vector $\boldsymbol{K}$ has only a single non-zero element. Therefore, instead of carrying out the matrix multiplication, the encoder may select the elements of χ at the specific positions corresponding to the non-zero element in $\boldsymbol{K}$. This reduces the decoding complexity imposed. As a result, the number of multiplications and the number of additions required for executing the decision matrix are equal to

$$C^{\times} = (4MT + 4MTNT + 2NT)QL, \quad (21)$$
$$C^{+} = [2MT + 2(2MT - 1)NT + 2JNT + 2NT - 1]QL. \quad (22)$$

Note that J denotes the number of taps describing our fading model, where the decoder has to eliminate the interfering signals dispersed from the previous symbol intervals. For a flat-fading channel, we have $J = 1$.

Since $\boldsymbol{K}$ host both the FSK symbol and the PSK/QAM symbol, the encoder requires additional multiplications and addition, which are quantified as

$$C^{\times} = 4QL, \quad (23)$$
$$C^{+} = 2QL. \quad (24)$$

Each STFSK block consists of $log_2(K \cdot Q \cdot L)$ bits. Hence, by employing Eqs. (19-24), the average number of multiplications, $\bar{C}^{\times}$, and the average number of additions, $\bar{C}^{+}$, required for each bit of a STFSK scheme is given by

$$\bar{C}^{\times} = \frac{2K + (4MT + 4MTNT + 2NT)QL + 4QL}{log_2(KQL)}, \quad (25)$$
$$\bar{C}^{+} = \frac{K + [2MT + 2(2MT + J)NT - 1]QL + 2QL}{log_2(KQL)} \quad (26)$$

2) STSK: STSK is a special case of STFSK, where $K = 1$, no FSK detector is necessary. Furthermore, the vector $\boldsymbol{K}$ now only contains PSK/QAM symbols. Hence, the average number of multiplications and additions for each bit of a STSK scheme may be reduced to

$$\bar{C}^{\times} = \frac{(4MT + 4MTNT + 2NT)QL}{log_2(QL)}, \quad (27)$$
$$\bar{C}^{+} = \frac{[2MT + 2(2MT + J)NT - 1]QL}{log_2(QL)}. \quad (28)$$

3) SFSK: Similarly, SFSK is another special case of STFSK, where we have $L = 1$ and the vector $\boldsymbol{K}$ now only hosts FSK symbols. Therefore, the average number of multiplications and additions for each bit of a SFSK scheme may be reduced to

$$\bar{C}^{\times} = \frac{2K + (4MT + 4MTNT + 2NT)Q}{log_2(KQ)}, \quad (29)$$
$$\bar{C}^{+} = \frac{K + [2MT + 2(2MT + J)NT - 1]Q}{log_2(KQ)}. \quad (30)$$

4) LDC: LDC is a special case of STSK, where we have $L = 1$. Thus, the vector $\boldsymbol{K}$ is redundant in the decision metric of Eq. (10). Hence, the the average number of multiplications and additions for each bit of a LDC scheme may be simplified to

$$\bar{C}^{\times} = \frac{(4MTNT + 2NT)QL}{log_2(QL)}, \quad (31)$$
$$\bar{C}^{+} = \frac{[2(2MT + J)NT - 1]QL}{log_2(QL)}. \quad (32)$$

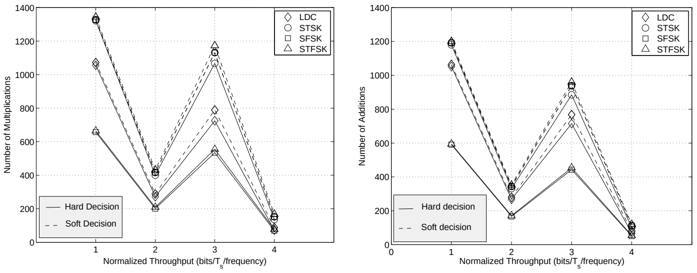

Fig. 3. Complexity versus the normalized throughput of the LDC, STSK, SFSK and STFSK schemes, where system parameters are provided in Table I.

B. Soft Demodulator

1) STFSK: In a soft STFSK demodulator each computation of Eq. (16) consists of two evaluations of Eq. (10) plus $log_2(QLK)$ multiplications and $log_2(QLK)$ additions rewired for adding the *a-priori* information. However, the searching space may be halved. Therefore, the average number of multiplications and additions becomes equivalent to

$$\bar{C}^{\times} = \frac{[4MT + 4MTNT + 2NT + 4 + log_2(QLK)]QLK}{log_2(QLK)}, \quad (33)$$

$$\bar{C}^{+} = \frac{[2MT + 2(2MT + J)NT + log_2(QLK)]}{log_2(QLK)}. \quad (34)$$

2) STSK: Similar to the hard-decision STSK demodulator, the soft-decision STSK demodulator only has to process PSK/QAM symbols. Hence, the average number of multiplications and additions for each bit of a STSK scheme may be reduced to

$$\bar{C}^{\times} = \frac{[4MT + 4MTNT + 2NT + log_2(QL)]QL}{log_2(QL)}, \quad (35)$$

$$\bar{C}^{+} = \frac{[2MT + 2(2MT + J)NT - 2 + log_2(QL)]}{log_2(QL)}. \quad (36)$$

3) SFSK: Similarly, the average number of multiplications and additions required for each bit of a soft-decision SFSK scheme, where $L = 1$, may be reduced to

$$\bar{C}^{\times} = \frac{[4MT + 4MTNT + 2NT + log_2(QK)]QK}{log_2(QK)}, \quad (37)$$

$$\bar{C}^{+} = \frac{[2MT + 2(2MT + J)NT - 2 + log_2(QK)]}{log_2(QK)}. \quad (38)$$

4) LDC: Finally, the average number of multiplications and additions associated with each bit of a soft-decision LDC scheme becomes

$$\bar{C}^{\times} = \frac{[4MTNT + 2NT + log_2(Q)]Q}{log_2(Q)}, \quad (39)$$

$$\bar{C}^{+} = \frac{[2(2MT + J)NT - 2 + log_2(Q)]}{log_2(Q)}. \quad (40)$$

The complexity results of the STFSK, STSK and SFSK schemes summarized in Table I are shown in Fig. 3, where the continuous and the dashed lines portray the detection complexity of the hard- and soft-demapper, respectively. As seen in the figure, the complexity of the hard-decision STFSK schemes is comparable to that of the SFSK schemes in terms of the number of multiplications and additions. By contrast, the hard-decision STSK schemes have doubled the complexity of the hard-decision STFSK and SFSK arrangements, when considering the same normalized throughput, while the number of multiplications and additions required by the hard-decision LDC demappers is 50% higher than those of the hard-decision STFSK schemes. Observe furthermore from Fig. 3 that the complexity of the soft-decision STSK, SFSK and STFSK demappers is comparable, while they are slightly more complex than the soft-decision LDC demapper. Furthermore, we found that in case of the SFSK and STFSK schemes the soft demappers doubled the complexity of the hard demappers, whilst in case of the STSK and LDC schemes the complexity of the soft- and hard-demappers remain comparable.

TABLE I
MODULATION SCHEMES' PARAMETERS

Parameters	$MNTQ$	L	K	Throughput
LDC	4/1/4/16	N/A	N/A	1 $bit/T_s/freq$
STSK	4/1/4/4	4	N/A	
SFSK	4/1/4/8	N/A	2	
STFSK	4/1/4/2	4	2	
LDC	4/1/2/16	N/A	N/A	2 $bit/T_s/freq$
STSK	4/1/2/4	4	N/A	
SFSK	4/1/2/8	N/A	2	
STFSK	4/1/2/4	2	2	
STSK	4/1/2/64	N/A	N/A	3 $bit/T_s/freq$
STSK	4/1/2/8	8	N/A	
SFSK	4/1/2/32	N/A	2	
STFSK	4/1/2/8	4	2	
LDC	4/1/1/16	N/A	N/A	4 $bit/T_s/freq$
STSK	4/1/1/4	4	N/A	
SFSK	4/1/1/8	N/A	2	
STFSK	4/1/1/4	2	2	

TABLE II
MODULATION SCHEMES' PARAMETERS

Scheme	$MNTQ$ $-L-K$	η	Hard-decision		Soft-decision	
			$C^{\times}$	C^{+}	$C^{\times}$	C^{+}
1	4/1/4/2-2-16	0.1875	227	201	3605	3221
2	4/1/4/2-4-8	0.375	445	397	3605	3221
3	4/1/4/2-8-4	0.75	887	793	3605	3221
4	4/1/4/2-16-2	1.5	1771	1584	3605	3221
5	4/1/4/4-2-8	0.375	455	397	3605	3221
6	4/1/4/4-4-4	0.75	887	793	3605	3221
7	4/1/4/4-8-2	1.5	1771	1584	3605	3221
8	4/1/4/8-2-4	0.75	887	793	3605	3221
9	4/1/4/8-4-2	1.5	1771	1584	3605	3221
10	4/1/4/16-2-2	1.5	1771	1584	3605	3221

Furthermore, the complexity of the hard- and the soft-decision STFSK schemes, where the block size of 6 bits per symbol is employed, is summarized in Table II. The following observations may be made:

- For the hard-decision, the complexity of decoder is reduced, when the number of frequencies, K, increases.
- For a given value of K and for a given value of the product QL, all possible combinations of Q and L exhibit the same decoding complexity when hard-decision is employed.
- in case of hard-decision, the complexity of a STFSK scheme increases upon increasing the normalized throughput.
- The complexity of a soft-decision STFSK demodulator depends only on the product of $(Q \times L \times K)$, rather than on each individual component Q, L and K.

V. PERFORMANCE RESULTS

In this section we consider the achievable iterative detection aided performance, when the soft STFSK demapper iteratively exchanges *extrinsic* information with the Recursive-Systematic-Convolutional (RSC) decoder. The RSC codec employs a half-rate constraint-length-3 code having the generator polynomial of $\frac{1+Z^{-2}}{1+Z^{-1}+Z^{-2}}$. The STFSK scheme is equipped with four transmit and a receive antenna, transmitting two symbols in four time slots $((M/N/T/Q = 4/1/4/2)$ and assisted by QPSK and BFSK. Observe from Fig. 4 that the achievable performance is significantly improved, when the number of iterations between the soft demapper and the RSC decoder was increased. Quantitatively, an E_b/N_0 improvement of 3 dB was achieved at the BER of 10^{-4}, when the number of iterations was increased from one to five.

The results of Fig. 4 are further supplemented by the EXIT charts. As seen in Fig. 5, at the E_b/N_0 value of -3 dB the intersection of the two EXIT curves is at the point of (0.75, 0.55) and up to this point a gradually narrowing tunnel exists between the two EXIT curves. Hence, at this value of E_b/N_0 only an insignificant improvement is obtained upon increasing the number of decoding iterations between the STFSK demodulator and the RSC decoder. By contrast, the tunnel is more widely open in case of $E_b/N_0 = -1$ dB in Fig. 5 and the $extrinsic$ information gleaned increases significantly, when the number of iterations increases from one to three. This explains why the attainable BER performance improves rapidly for the first three iterations, while the BER improvement significantly reduces for the fourth and fifth iteration.

Fig. 6 characterizes the performance of all the ten STFSK schemes of Table II. The performance confirms the EXIT-chart based prediction of Fig. 2. More particularly, the results may be divided into four groups. The first group, including Schemes $\{1,2,3\}$, exhibit the best performance, achieving a BER of 10^4 at an E_b/N_0 value around 0 dB. The EXIT functions of the demappers in these three schemes are shown at top of Fig. 2, where a significant advantage is shown in comparison to the remaining schemes. The second group consisting Schemes $\{4,5,6,7\}$ achieved the same BER, namely 10^4, at the E_b/N_0 of about 2.5 dB. The EXIT functions of these schemes remained significantly below those of the first group. The third group contained Scheme 8 and Scheme 9, whose EXIT functions remained further below those of Schemes $\{4,5,6,7\}$ in Fig. 2. They achieved the BER of 10^4 at the E_b/N_0 value around 5.5 dB. Finally, Scheme 10, which has the demapper EXIT function at the bottom of Fig. 2, acquired the same BER at the E_b/N_0 value around 9.5 dB.

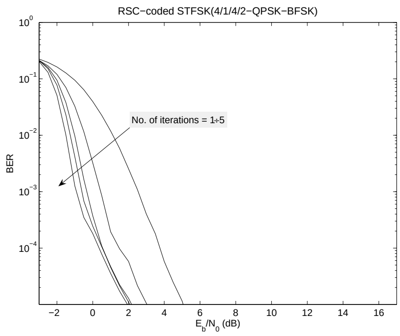

Fig. 4. The performance of the soft-detected RSC-coded STFSK(4/1/4/2) with the aid of QPSK and BFSK modulations.

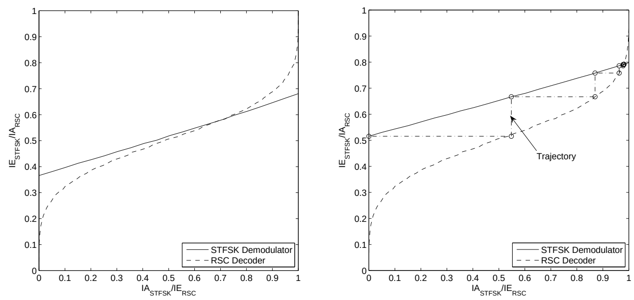

Fig. 5. EXIT Charts of the RSC coded STFSK using Iterative Decoding at $E_b/N_0 = -3$ dB (left) and -1 dB (right).

VI. Conclusions

In this paper we proposed the soft-modulation aided iterative decoding of STFSK. Our results demonstrated that upon carrying out iterative information exchange between the STFSK soft-demodulator and the RSC channel decoder, the system achieved a 3 dB power gain at the E_b/N_0 value of 10^{-5} compared to using its counterpart dispensing with iterative decoding. Also, we quantified the detection complexity of both the hard- and soft-detection STFSK demodulators.

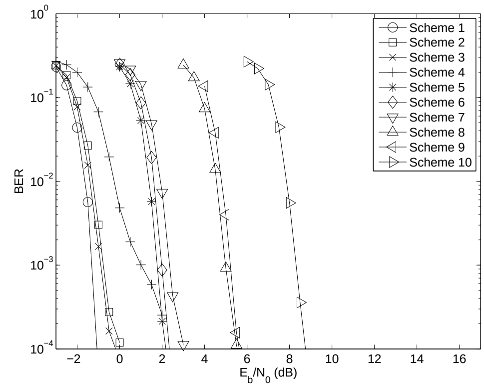

Fig. 6. The performance of the soft-decision RSC-coded STFSK schemes of Table II, where the EXIT functions of STFSK demodulators at $E_b/N_0 = 0$ dB is shown in Fig. 2.

References

[1] S. M. Alamouti, "A simple transmit diversity technique for wireless communications," *IEEE Journal on Selected Areas in Communications*, vol. 16, no. 8, pp. 1451–1458, 1998.

[2] V. Tarokh, N. Seshadri, and A. R. Calderbank, "Space-time codes for high data rate wireless communication: Performance criterion and code construction," *IEEE Transaction on Information Theory*, vol. 44, pp. 744–765, 1998.

[3] V. Tarokh, H. Jafarkhani, and A. R. Calderbank, "Space-time block codes from orthogonal designs," *IEEE Transactions on Information Theory*, vol. 45, no. 5, pp. 1456–1467, 1999.

[4] V. Tarokh, A. Naguib, N. Seshadri, and A. R. Calderbank, "Space-time codes for high data rate wireless communication: performance criteria in the presence of channel estimation errors, mobility, and multiple paths," *IEEE Transactions on Communications*, vol. 47, no. 2, pp. 199–207, 1999.

[5] B. Hochwald, T. L. Marzetta, and C. B. Papadias, "A transmitter diversity scheme for wideband cdma systems based on space-time spreading," *IEEE Journal on Selected Areas in Communications*, vol. 19, no. 1, pp. 48–60, 2001.

[6] G. J. Foschini, "Layered space-time architecture for wireless communication in a fading environment when using multi-element antennas," *Bell Laboratories Technical Journal*, vol. 1, pp. 41–59, 1996.

[7] P. W. Wolniansky, G. J. Foschini, G. D. Golden, and R. A. Valenzuela, "V-BLAST: an architecture for realizing very high data rates over the rich-scattering wireless channel," in *Proceedings of URSI International Symposyum on Signals, Systems, and Electronics - ISSSE'98*, pp. 295–300, 1998.

[8] B. Hassibi and B. M. Hochwald, "High-rate codes that are linear in space and time," *IEEE Transactions on Information Theory*, vol. 48, no. 7, pp. 1804–1824, 2002.

[9] R. Y. Mesleh, H. Haas, S. Sinanovic, C. W. Ahn, and S. Yun, "Spatial modulation," *IEEE Transactions on Vehicular Technology*, vol. 57, no. 4, pp. 2228–2241, 2008.

[10] J. Jeganathan, A. Ghrayeb, L. Szczecinski, and A. Ceron, "Space shift keying modulation for MIMO channels," *IEEE Transactions on Wireless Communications*, vol. 8, no. 7, pp. 3692–3703, 2009.

[11] S. Sugiura, S. Chen, and L. Hanzo, "Coherent and differential space-time shift keying: A dispersion matrix approach," *IEEE Transactions on Communications*, vol. 58, pp. 3219–3230, Nov. 2010.

[12] G. Leus, W. Zhao, G. B. Giannakis, and H. Delic, "Space-time frequency-shift keying," *IEEE Transactions on Communications*, vol. 52, no. 3, pp. 346–349, 2004.

[13] H. A. Ngo, C. Xu, S. Sugiura, and L. Hanzo, "Space-time-frequency shift keying for dispersive channels," *IEEE Signal Processing Letters*, vol. 18, no. 3, pp. 177–180, 2011.

[14] J. G. Proakis, *Digital communications*. McGraw-Hill, 4th ed., 2001.

[15] J. Jeganathan, A. Ghrayeb, and L. Szczecinski, "Spatial modulation: optimal detection and performance analysis," *IEEE Communications Letters*, vol. 12, no. 8, pp. 545–547, 2008.

[16] S. ten Brink, "Convergence behavior of iteratively decoded parallel concatenated codes," *IEEE Transactions on Communications*, vol. 49, no. 10, pp. 1727–1737, 2001.

[17] L. Hanzo, O. Alamri, M. El-Hajjar, and N. Wu, *Near-Capacity Multi-Functional MIMO Systems: Sphere-Packing, Iterative Detection and Cooperation*. John Wiley - IEEE Press, May 2009.